

# An Improved Heuristic UTD Solution for Multiple-Edge Transition Zone Diffraction

Constantinos Tzaras and Simon R. Saunders, *Member, IEEE*

**Abstract**—This paper describes a new heuristic approach for multiple edge diffraction modeling based on the uniform theory of diffraction (UTD). It incorporates the slope diffraction terms which can be realized as a second-order diffraction process, vital for accurate predictions when more than one edge exists. The predictions of this approach are compared with the Vogler solution and were found to be in very good agreement for many different geometrical arrangements, with low computational complexity. The solution is also extended to wedge diffraction.

**Index Terms**—Geometrical theory of diffraction, propagation modeling.

## I. INTRODUCTION

MODERN services, such as digital video broadcasting and cellular communication systems, have led to the development of powerful theoretical deterministic models for the prediction of field strengths over paths of given profile [1], [4]–[6]. Due to the widespread use of radio frequencies of wavelengths, small compared with the major terrain irregularities, obstacles are commonly treated as knife-edges, with wedges and cylinders used for increased accuracy. This representation has been found appropriate for built-up areas [7], with the Vogler solution [4] representing the ultimate in accuracy compared with other approximate deterministic models (e.g., [1], [6]).

A common feature of all multiple knife-edge diffraction models is that there is a trade-off between accuracy and computation speed. Methods that are characterized by small computation times are unable to estimate the received signal strength with great accuracy and vice versa. Although, the Vogler solution can offer very accurate results, the complexity in computational requirements makes it prohibitive, especially when area coverage predictions are needed, although recent work has shown how to minimize the time [8]. A new approach has been presented in [1], which couples small computation times with fairly accurate predictions. The formulas in [1] perform much better in accuracy than the original first-order UTD solutions in [9], proving that the slope diffraction term is a critical component for accurate diffraction predictions. However, the predictions of this heuristic approach still suffer from inaccuracies, especially when the number of edges increases or the edges have unequal heights. A more accurate UTD solution has been studied in [5], but the diffraction process involves

Manuscript received September 9, 1999; revised September 6, 2000. This work was supported by the UK Engineering and Physical Sciences Research Council under the LINK Project DigiPlan, the British Broadcasting Corporation, Cellular Design Services Ltd. and Ericsson Radio Systems.

The authors are with the Centre for Communication Systems Research, University of Surrey, Guildford, Surrey GU2 5XH U.K.

Publisher Item Identifier S 0018-926X(01)07652-9.

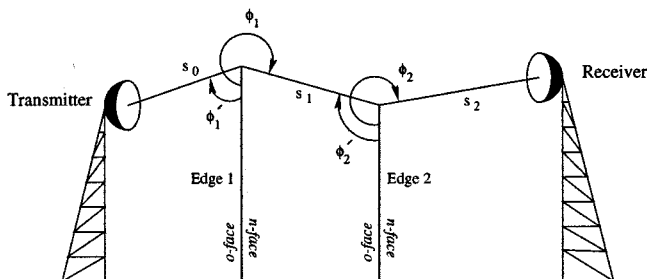


Fig. 1. Ray geometry for multiple knife-edge diffraction.

computation of many higher order terms whose number cannot be predicted for a particular path profile. The present study explores and improves the heuristic approach presented in [1], maintaining the simplicity of the method, while producing more accurate predictions with low computation times. Detailed simulations are quoted in order to illustrate the new formulation and compare it with other methods.

## II. BASIC THEORY

According to the UTD theory [2], the diffracted field for a single absorbing knife-edge is given by

$$E = \left[ E_i D(\alpha) + \frac{\partial E_i}{\partial n} d_s(\alpha) \right] A(s) e^{-jks} \quad (1)$$

where

- $\alpha \equiv \phi - \phi'$ ;
- $\phi$  diffraction angle with respect to the *o*-face of the edge;
- $\phi'$  incident angle with respect to the *o*-face of the edge (Fig. 1);
- $A(s)$  spreading factor

$$A(s) = \sqrt{\frac{s_0}{s(s+s_0)}}. \quad (2)$$

The amplitude diffraction coefficient  $D(\alpha)$  is given by

$$D(\alpha) = -\frac{e^{-j\pi/4}}{2\sqrt{2\pi k} \cos(\alpha/2)} F[2kL \cos^2(\alpha/2)] \quad (3)$$

whereas, the slope diffraction coefficient is given by

$$d_s(\alpha) = \frac{1}{jk} \frac{\partial D(\alpha)}{\partial \alpha}. \quad (4)$$

The term  $F(x)$  is known as the transition function

$$F(x) = 2j\sqrt{x}e^{jx} \int_{\sqrt{x}}^{\infty} e^{-ju^2} du \quad (5)$$

and the derivative of this function is

$$F'(x) = j[F(x) - 1] + \frac{F(x)}{2x}. \quad (6)$$

According to (4), (6), the slope diffraction coefficient is given by

$$d_s(\alpha) = -\frac{e^{-j\pi/4}}{\sqrt{2\pi k}} L_s \sin(\alpha/2)(1 - F(x)) \quad (7)$$

and its derivative by

$$\frac{\partial d_s(\alpha)}{\partial n} = -\frac{1}{2s} \frac{e^{-j\pi/4}}{\sqrt{2\pi k}} \{L_s \cos(\alpha/2)[1 - F(x)] + 4L_s^2 k \sin^2(\alpha/2) \cos(\alpha/2) F'(x)\}. \quad (8)$$

The contribution of [1] was that the  $L$  and  $L_s$  parameters in (3) and (7) were calculated according to some continuity equations, which ensure continuity of the diffracted field and its slope along the shadow boundaries of the edges.

The innovation in the approach presented here is to develop different continuity equations which vary for each ray independently. Hence, the values of  $D(\alpha)$  and  $d_s(\alpha)$  are different for each ray, even if the diffracted edge and the receiver point are the same. Although such an approach results in a little added complexity, this method produces more accurate output compared to [1] as will be noticed in later example calculations. Furthermore, the present approach is thought to be more physically correct, since both the magnitude and the phase of the signal are taken into account when the  $L$  and  $L_s$  parameter values are calculated.

### III. DOUBLE AND TRIPLE KNIFE-EDGE DIFFRACTION

In this section, two and three knife-edges colinear with the transmitter and the receiver, and arbitrary spacing are considered (Fig. 2). It is assumed that the slope of the field is zero only when it originates from the transmitter. Hence, denoting the total field at edge  $m$  by  $E_m$  and the field at edge  $m$  due to edge  $n$  as  $E_{nm}$ , the total field on the second edge is

$$E_2 = E_{02} + E_{01}D_1(\alpha_{012})A_1(s_1)e^{-jks_1} \quad (9)$$

where

- $E_{02}$  incident field from the source;
- $E_{01}$  incident field from the source at edge 1;
- $\alpha_{012}$  comprises the transmitter, the first, and the second edge.

The continuity equation for evaluating the  $L$  parameter that appears in  $D_1(\alpha)$  is

$$0.5E_{02} = E_{01}D_1(\alpha_{012})A_1(s_1)e^{-jks_1}. \quad (10)$$

For  $\alpha = \pi$ , the amplitude diffraction coefficient is given by

$$D(\pi) = 0.5\sqrt{L}. \quad (11)$$

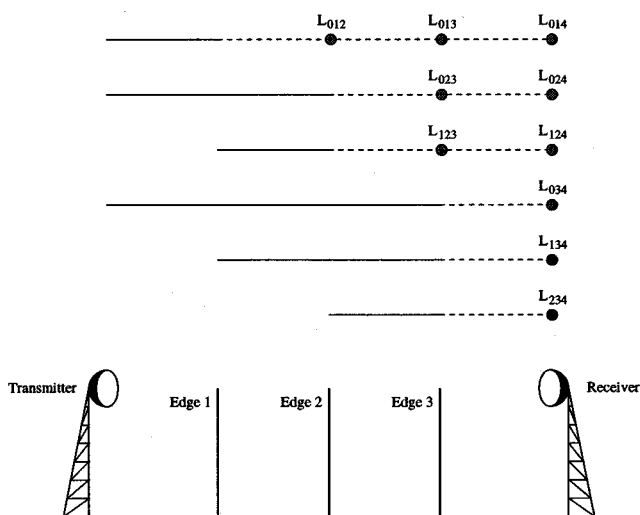


Fig. 2. Path geometry for 3 knife-edges with equal heights and spacings. The index of each  $L$  parameter refers to the edge where the ray originates, amplitude diffracted and received.

Hence, following (10)

$$\frac{0.5}{s_0 + s_1} e^{-jk(s_0 + s_1)} = \frac{0.5}{s_0} e^{-jks_0} \sqrt{L_{012}} \sqrt{\frac{s_0}{s_1(s_0 + s_1)}} e^{-jks_1}$$

from which

$$L_{012} = \frac{s_0 s_1}{s_0 + s_1}. \quad (12)$$

The total field at edge 2 is then

$$E_2 = \frac{0.5}{s_0 + s_1} e^{-jk(s_0 + s_1)}. \quad (13)$$

The present approach differs from [1] when the field at edge 3 and after, need to be calculated. First, the  $L$  parameters for the second edge need to be evaluated. The continuity equations for amplitude diffraction are

$$0.5E_{03} = E_{01}D_1(\alpha_{013})A_1(s_1 + s_2)e^{-jk(s_1 + s_2)} \quad (14a)$$

$$0.5E_{03} = E_{02}D_2(\alpha_{023})A_2(s_2)e^{-jks_2} \quad (14b)$$

$$0.5E_{13} = E_{12}D_2(\alpha_{123})A_2(s_2)e^{-jks_2}. \quad (14c)$$

From (14a)

$$L_{013} = \frac{s_0(s_1 + s_2)}{s_0 + s_1 + s_2}. \quad (15)$$

From (14b),

$$L_{023} = \frac{(s_0 + s_1)s_2}{s_0 + s_1 + s_2}. \quad (16)$$

Finally, from (14c)

$$L_{123} = \frac{(s_0 + s_1)s_2}{s_0 + s_1 + s_2}. \quad (17)$$

As can be noticed, the parameters  $L_{023}$  or  $L_{123}$  do not have the same form as  $L_{012}$  or  $L_{013}$ , contrary to the assumption in [1] where all these terms have similar formulation with  $L_{012}$

or  $L_{013}$ . This effect becomes more significant as the number of edges increases or if the edges have very different heights.

Finally, for the slope term

$$\begin{aligned} \frac{\partial E_2}{\partial n} &= E_{01} \frac{\partial D(\alpha_{012})}{s_1 \partial \alpha_{012}} A_1(s_1) e^{-jk s_1} \\ &= E_{01} \frac{jk d_s(L_{012})}{s_1} A_1(s_1) e^{-jk s_1} \\ &= \frac{e^{j\pi/4}}{\sqrt{2\pi}} \sqrt{k} \sqrt{\frac{s_0}{s_1}} \frac{1}{(s_0 + s_1)^{3/2}} e^{-jk s_1}. \end{aligned} \quad (18)$$

Following the same continuity equation as [1] for the slope term, the  $L_s$  parameter is

$$L_s = \left( \frac{s_0 + s_1}{s_0 + s_1 + s_2} \right)^{2/3} \left( \frac{s_1}{s_1 + s_2} \right)^{1/3} s_2. \quad (19)$$

Although, the  $L_s$  parameter is the same as that calculated in [1], it produces different values when more than two edges exist in the propagation path.

The total field at edge 3 is then

$$\begin{aligned} E_3 &= E_{03} + E_{01} D_1(\alpha_{013}) A_1(s_1 + s_2) e^{-jk(s_1 + s_2)} \\ &\quad + [E_{02} D_2(\alpha_{023}) + E_{12} D_2(\alpha_{123})] A_2(s_2) e^{-jk s_2} \\ &\quad + \frac{\partial E_2}{\partial n} d_s(\alpha_{123}) A_2(s_2) e^{-jk s_2}. \end{aligned} \quad (20)$$

Hence

$$\begin{aligned} E_3 &= \frac{0.25}{s_0 + s_1 + s_2} e^{-jk(s_0 + s_1 + s_2)} \\ &\quad + \frac{1}{2\pi} \sqrt{\frac{s_0}{s_1}} \frac{L_s}{(s_0 + s_1)^{3/2}} A_2(s_2) e^{-jk(s_0 + s_1 + s_2)}. \end{aligned} \quad (21)$$

As can be noticed, for only two edges with equal heights, (21) is the same as [1, eq. (16)]. However, for more than two edges, the solution of the present approach is more close to the correct result [3] as will be shown in the next section.

#### IV. MULTIPLE KNIFE-EDGE DIFFRACTION

Following the results in the previous section, the proposed method can easily be extended to three knife-edges and then by recursion to  $N$  knife-edges. For each edge there will always exist an amplitude diffraction term and a slope diffraction term. The  $L$  and  $L_s$  values need to be calculated according to the continuity equations which must be formed for each ray independently.

Hence, the field at edge 4 (Fig. 4) will be given by

$$E_4 = E_{\text{absent},3} + \left[ E_3 D_3(\alpha) + \frac{\partial E_3}{\partial n} d_3(\alpha) \right] A_3(s_3) e^{-jk s_3} \quad (22)$$

where  $E_4$  is the total field at edge 4,  $E_{\text{absent},3}$  is the field at edge 4 with edge 3 absent, resulting in a two-edge diffraction problem. The term  $E_3 D_3(\alpha)$  is analyzed for all the components of the field at edge 3 since the diffraction coefficient could possess different values for different rays. Finally, the same concept

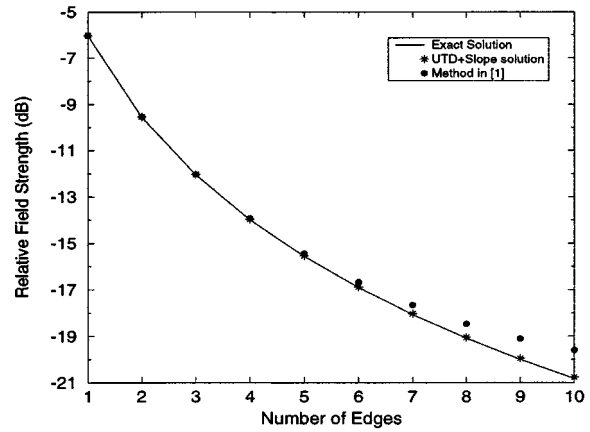


Fig. 3. Relative field strength versus number of knife-edges for equal heights and spacings.

should be followed for the term  $(\partial E_3 / \partial n) d_3(\alpha)$ , where for this term an additional calculation to find the derivative of the slope diffraction coefficient is made, as given by (8).

A recursive computer algorithm has been implemented to illustrate the performance of this heuristic approach. As illustrated in Fig. 3, for nine edges, the method in [1] exhibits an error of approximately 1 dB whereas in our case, the error is only 0.04 dB. In addition, the method proposed in [1] diverges more rapidly from the correct result as the number of edges increases, significantly overestimating the relative path loss.

Although the present method is more complicated than [1], it is still very easy to implement in a recursive computer algorithm with fast computation times if compared with [4].

#### V. UNEQUAL HEIGHTS AND SPACINGS

When the edges have different heights, the  $L$  and  $L_s$  parameters are determined as previously, although different path profiles have to be considered. An unjustified constraint of [1] is that for unequal heights, only the magnitude of the signal is considered in every continuity equation. If the phase is also included, the equations do not give an acceptable value. Such a practice might suggest that the heuristic approach in [1] cannot be physically correct, since the magnitude alone is not enough to evaluate correctly each  $L$  or  $L_s$  parameter. However, in the present approach, both the magnitude and the phase are taken into account. Since the continuity equations are valid only when the origin of the ray, the diffracting edge and the field point lie on the shadow boundary, new field points need to be found. Since the continuity equations are valid only when the origin of the ray, the diffracting edge and the field point lie on the shadow boundary, new field points need to be found. Fig. 4 illustrates how these receiver points are calculated, whose total number is  $(N - i + 1)$  for edge  $i$ , where  $N$  is the total number of edges. Assuming that a line-of-sight case exists for all the edges, the total number of  $L$  parameters is  $i(N - i + 1)$ , whereas the total number of  $L_s$  parameters is  $(i - 1)(N - i + 1)$ .

In Fig. 5, the output is compared with [4, Fig. 2] with a very good agreement whereas the method in [1] exhibits a maximum error of approximately 0.7 dB. In addition, when the middle edge does not exist, both the Vogler solution and the present

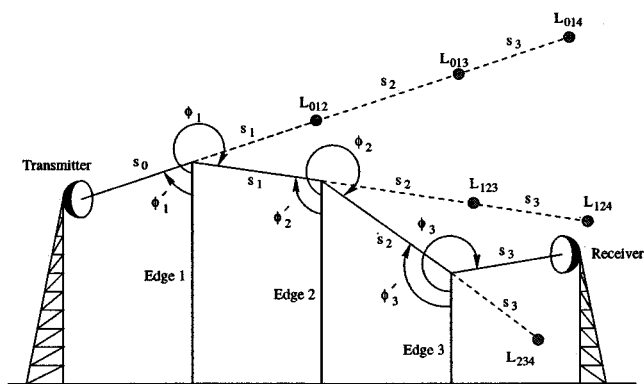


Fig. 4. Path geometry for three knife-edges with unequal heights and spacings.

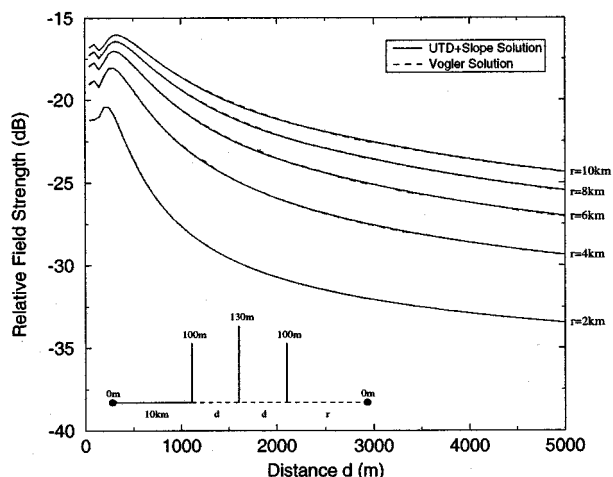


Fig. 7. Relative field strength versus spacing. The output agrees exceptionally well with the Vogler solution.

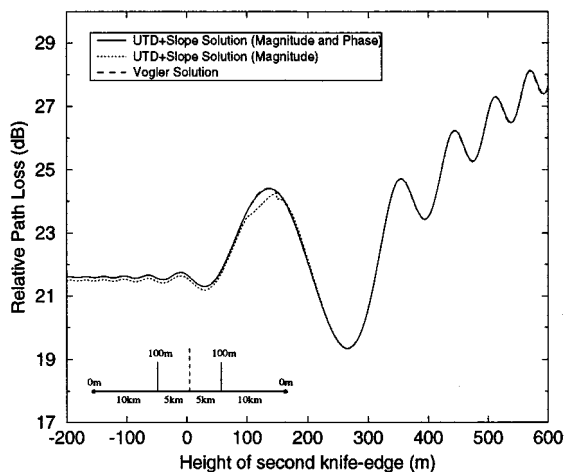


Fig. 5. Comparison with [1, Fig. 7(b)] and [4, Fig. 2]. The output agrees exceptionally well with the Vogler solution.

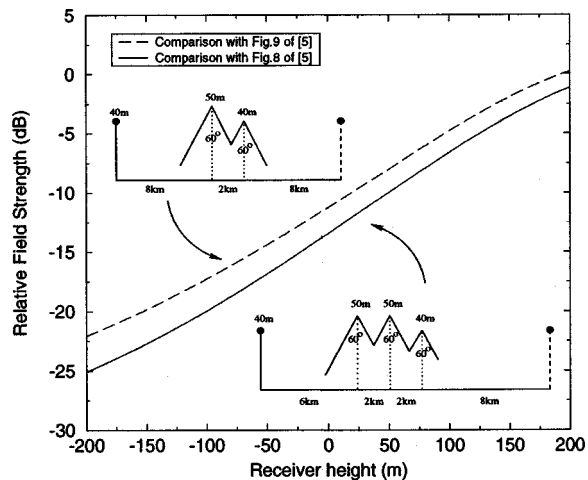


Fig. 8. Comparison with [5, Figs. 8 and 9]. The output agrees exceptionally well with the higher-order solution.

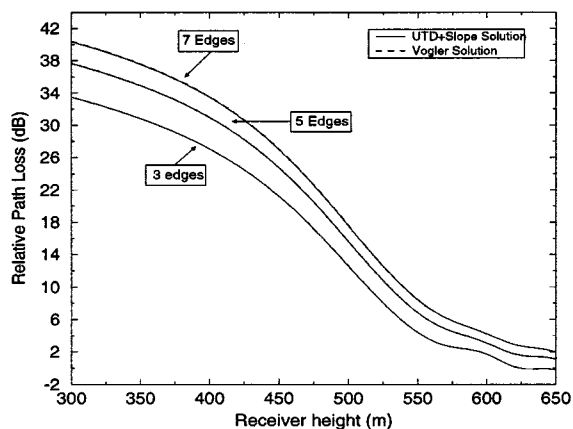


Fig. 6. Comparison with [4, Fig. 3]. The output agrees exceptionally well with the Vogler solution.

method find similar path loss (21.6 dB) whereas the solution in [1] exhibits an error of approximately 0.1 dB.

Another important feature in Fig. 5 is that the evaluation of the  $L$  parameters when only the magnitude of the field is considered results to large errors, as practiced in [1].

In Fig. 6, the output is compared with [4, Fig. 3] with an excellent agreement, whereas Fig. 7 shows another example calculation for three edges at 100 MHz with equal distances between

the first and second edge and also between the second and third edge. In this figure, different curves correspond to different distances between the final edge and the receiver. As previously, the method agrees very well if compared with the Vogler solution. However, even the present approach does not produce the correct predictions when the relative distances are very small compared to the total path length (less than 50 m spacing in Fig. 7), an effect which is inherited from the original UTD solution.

### VI. APPLICATION TO WEDGES

The same approach may also be applied to conducting or reflecting wedges by considering the appropriate formulas that exist in the literature for the UTD solution [2].

In the case of perfectly conducting wedges, (3), (7), and (8) need to be modified to account for the interior wedge angle.

Fig. 8 shows an example calculation with two and three perfectly conducting wedges of interior angle  $60^\circ$  at a frequency of 100 MHz with horizontal polarization. It can be seen that the present approach agrees very well with [5, Figs. 8 and 9]. However, the output in Fig. 8 may also be found if a knife-edge

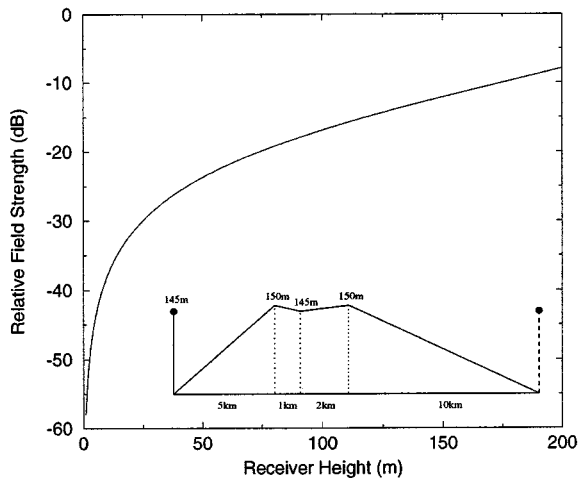


Fig. 9. Comparison with [5, Fig. 10] for two wedges. The output agrees exceptionally well with the higher-order solution.

configuration is used, due to the small interior wedge angle. A calculation that is more representative of the proposed UTD solution can be viewed in Fig. 9, where the results can be obtained only for a wedge configuration. The path profile is similar to [5, Fig. 10] for two wedges, assuming horizontal polarization. Once again, it can be noticed that it agrees very well with the results in [5], although the order of the solution is much less than the one proposed in [5].

## VII. CONCLUSION

A modified heuristic UTD solution was presented here in comparison with a previous solution [1]. The results were characterized by rapid computation time and very good accuracy if compared with well known solutions [4], [5], even though a second order UTD solution was employed in contrast with [5]. In addition to knife-edge configurations, the method was also applied to wedges where the results verified the validity of this approach. However, the method inherits a deficiency of the UTD solution, as it cannot predict the correct diffraction loss when two edges are very close to each other. Fortunately, this effect is geometry dependent and does not appear in all cases where there are very short separation distances.

## REFERENCES

- [1] J. B. Andersen, "UTD multiple-edge transition zone diffraction," *IEEE Trans. Antennas Propagat.*, vol. 45, pp. 1093–1097, July 1997.
- [2] D. A. McNamara, C. W. I. Pistorius, and J. A. G. Malherbe, *Introduction to the Uniform Geometrical Theory of Diffraction*. Norwood, MA: Artech House, 1990.
- [3] S. W. Lee, "Path integrals for solving some electromagnetic edge diffraction problems," *J. Math. Phys.*, vol. 19, pp. 1414–1422, 1978.
- [4] L. Vogler, "An attenuation function for multiple knife-edge diffraction," *Radio Sci.*, vol. 17, pp. 1541–1546, 1982.
- [5] P. D. Holm, "UTD diffraction coefficients for higher order wedge diffracted fields," *IEEE Trans. Antennas Propagat.*, vol. 44, pp. 879–888, June 1996.

- [6] J. Deygout, "Multiple knife-edge diffraction of microwaves," *IEEE Trans. Antennas Propagat.*, vol. AP-14, pp. 480–489, 1966.
- [7] S. R. Saunders and F. R. Bonar, "Prediction of mobile radio wave propagation over buildings of irregular heights and spacings," *IEEE Trans. Antennas Propagat.*, vol. 42, pp. 137–144, Feb. 1994.
- [8] C. Tzaras and S. R. Saunders, "Rapid, uniform computation of multiple knife-edge diffraction," *Inst. Elect. Eng. Electron. Lett.*, vol. 35, pp. 237–239, Feb. 1999.
- [9] R. G. Kouyoumjian and P. H. Pathak, "A uniform geometrical theory of diffraction for an edge in a perfectly conducting surface," *Proc. IEEE*, vol. 62, pp. 1448–1461, Nov. 1974.



**Constantinos Tzaras** received the B.Sc. degree in physics from Aristotle University of Thessaloniki, Greece, in 1995. He received the M.Sc. degree and the Ph.D. degree, both in electrical engineering, from the University of Surrey in 1997 and 2001, respectively.

He is currently with Vodafone U.K., as a Radio Modeling Engineer, innovating technology for cellular systems. Formerly, he was a Research Fellow with the University of Surrey, specializing in cellular and broadcasting radio communications. During this time, he received four separate awards for academic and research excellence. His research interests include wireless communication systems.



**Simon R. Saunders** (S'89–M'91) received the B.Sc. degree (1st Class Honors) and the Ph.D. degree at Universiti Brunei Darussalam, Brunei, in 1988 and 1991, respectively.

Since 1996, he has been with The University of Surrey, in Guildford, U.K., at the Centre for Communication Systems Research where he is a Reader. In 1991, he was a Research Fellow with Universiti Brunei, working on microwave oscillator structures. He also received four separate awards for academic achievement during his time Universiti Brunei. He was with Philips Telecom, in Cambridge, U.K., as a Senior Engineer for several years innovating technology for private mobile and paging systems. He was also a Philips' Telecom representative on the ETSI committee responsible for defining and standardizing the air interface of the new TETRA European digital standard for trunked Private Mobile Radio. He led a team investigating systems issues and designing technology for a novel two-way paging system, founded on the POCSAG standard, involving particular challenges connected with modulation methods, access schemes, system architecture and equipment design. In 1995, he was with Motorola GSM Research Group, designing air interface and system planning enhancements leading to increased capacity second generation GSM systems. This included advances in antenna, modem and cellular architectures and led to the origination of thirteen patent proposals. From 1993 to 1994, he proposed a novel parallel approach to the solution of electromagnetic problems, acted as consultant to the resulting project, which led to the creation of an electromagnetic simulation package, intended for use as a CAD and teaching tool. He spent one year working with the Ascom Tech Mobile Radio Research Group in Switzerland, defining product technologies and system design solutions for a new digital mobile radio system. He has authored of over 50 papers in learned journals and international conferences. He is also author of *Antennas and Propagation for Wireless Communication Systems*, (New York: Wiley, 1999). Research interests include center improving understanding of the mobile radio propagation channel and mobile system air interface design methods. Specific research areas are: antennas for satellite and terrestrial mobile handsets; intelligent antennas for high-capacity terrestrial mobile systems; propagation measurements and prediction models for terrestrial and satellite mobile systems.